

# Ramsey interferometry in three-level and five-level systems of $^{87}\text{Rb}$ Bose-Einstein condensates

Anushka Thenuwara<sup>1,2</sup>, Andrei Sidorov<sup>1</sup>

<sup>1</sup> Centre for Optical Sciences, Faculty of Science, Engineering and Technology, Swinburne University of Technology, John Street, Hawthorn, Victoria, Australia 3122

<sup>2</sup> School of Physics and Astronomy, Monash University Clayton Campus, Wellington Rd, Clayton, Victoria, Australia 3800

E-mail: anushka.thenuwara@monash.edu and asidorov@swin.edu.au

July 2021

**Abstract.** Our work here presents the analytical expressions for a typical Ramsey interferometric sequence for a three- and a five-level system. The analytical expressions are derived starting from the first principals of unitary time evolution operators. We focus on the three- and five-level systems because we propose a novel Ramsey interferometer created by a trapped two-state Bose-Einstein Condensate driven by dipole oscillations and gravitational sag. It involves the  $^{87}\text{Rb}$  atoms in states  $|F = 2, m_F = +2\rangle$  ( $|+2\rangle$ ) and  $|F = 2, m_F = +1\rangle$  ( $|+1\rangle$ ) of the  $5^2S_{1/2}$  ground state. Though the interferometer focusses on the two-levels, the experimental readouts involve all the five states in  $F = 2$  hyperfine manifold. Therefore, the analytical derivation was first tested for three-levels and then expanded to five-levels. We developed the expressions for five-levels for greater analytical accuracy of the experimental scenario. This work provides a step-by-step outline for the derivation and methodology for the analytical expressions. These analytical formulae denote the population variation during Rabi and Ramsey oscillations for each state as well as the overall average for both the three- and five-level cases. The expressions are derived within the rotating wave approximation (RWA) under the equal Rabi condition. Further, by following the derivation methodology, these analytical expressions can be easily expanded for Ramsey sequences with unequal pulses, and Ramsey sequences with spin echo techniques.

## 1. Introduction

Following the work of I.I. Rabi, N.F. Ramsey [1] significantly improved the Rabi method by using two oscillatory fields with a short pulse  $\tau$  separated by a long free evolution time  $T$  to study molecular resonances and demonstrated 0.6 times narrower linewidths. This work of N.F. Ramsey won him the Nobel prize in physics in 1989 and is named as Ramsey interferometry. This method provides the basis of the exquisite time standards of  $\text{Cs}$  fountain clocks such as the NIM5 clock in China and the NIST-F1 in the USA that have uncertainties of  $1.6 \times 10^{-15}$  [2] and  $0.97 \times 10^{-15}$

[3] respectively. Further, Ramsey interferometry allows sensitive measurements of local gravity [4] and a Ramsey-type method with a spin-echo pulse (i.e. a  $\pi$ -pulse during the free evolution time  $T$ ) allows precise measurements of the Newtonian gravitational constant  $G = 6.671\,91(99) \times 10^{-11} \text{ m}^3\text{kg}^{-1}\text{s}^{-2}$  [5]. This applied in multilevel systems allows to measure below the standard quantum limit [6] where the phase difference between states are mapped onto the populations of states [7].

The primary goal of this work is to develop analytical expressions to explore and analyse experimental data of a novel Ramsey interferometer created by a trapped two-state Bose-Einstein condensate (BEC) driven by dipole oscillations and gravitational sag. A BEC is formed in a pure compressed magnetic trap (CMT) via a cloud of  $^{87}\text{Rb}$  atoms in state  $|F = 2, m_F = +2\rangle$  ( $|+2\rangle$ ) of the  $5^2S_{1/2}$  ground state, from which Ramsey interferometry is performed between states  $|+2\rangle$  and  $|F = 2, m_F = +1\rangle$  ( $|+1\rangle$ ). The state  $|+1\rangle$  experiences a shallower radial trap with a larger gravitational sag; whereas, state  $|+2\rangle$  experiences a tighter radial trap with a gravitational sag that is half of state  $|+1\rangle$ . Due to this, a superposition between the states  $|+1\rangle$  and  $|+2\rangle$  experiences multipath propagation resulting in an interference pattern. This may be utilised to measure local gravitational fields and measure inter-state scattering lengths.

In previous works [8, 9, 10, 11] analytical expressions for Rabi oscillations in multi-level system were attained based on the two-level atom (Equation 12). In [8] considers an N-level atom interacting with a near-resonant laser field in two fronts; where the energy separation between all N-states are equal (equal-Rabi), and the energy separation increases as a harmonic potential (harmonic-Rabi). It also shows the association with Chebyshev and Hermite polynomials. The work in [9] incorporates the treatment of losses and [12, 13, 14] shows the importance of understanding Rabi oscillations of a multi-level system for quantum computation. These formulations are performed within the rotating wave approximation (RWA) which is valid when the coupling constant (Rabi frequency) is much smaller than the energy separation between the two levels [12]. In this work we derive analytical expressions for a three- and five-level systems for the full Ramsey sequence via the unitary time evolution operator formalism under the equal-Rabi and RWA conditions.

The equal-Rabi assumption is valid as the trap bottom of the harmonic oscillator potential of the experiment is about 1 G relating to about 700 kHz energy separation between the five states in the  $F = 2$  hyperfine manifold [15]. The Breit-Rabi formula [16, 17] indicates there is only a 0.02% variation in energy between adjacent states spanning  $|+2\rangle$  to  $|-2\rangle$ . Due to this the equal-Rabi model suffices and the harmonic-Rabi model only complicates the analysis. Further, the maximum experimental Rabi frequency is less than 15% of that of the energy separation between states which justifies the RWA approximation.

Within these considerations, Section 2 derives the analytical expressions for the unitary time evolution  $\hat{U}$  for the three-level system via  $\hat{U} = \sum_{i=1}^n e^{\frac{-i\lambda_i t}{\hbar}} |V_i\rangle \langle V_i|$  (Equation 3), where  $\lambda_i$  are the eigenvalues and  $|V_i(t)\rangle$  are the eigenvectors of the interaction Hamiltonian  $\hat{H}_I$ . Once the methodology is validated, analytical expressions

for the five-level system are derived and presented in Section 3. Mathematica was used to solve these analytically dense problems.

## 2. Rabi and Ramsey analytical models for three-level system

Consider a three-level system with equal energy separation between adjacent states leading to  $\omega_{|+1\rangle} - \omega_{|0\rangle} = \omega_{|0\rangle} - \omega_{|-1\rangle} = \omega_{Sep}$  being coupled to an external EM field with a frequency  $\omega_{EM} = \omega_{Sep} - \Delta$  where  $\Delta$  is the detuning. The Rabi frequency for this system follows the resonant Rabi frequency  $\Omega_R$  in Equation ?? where  $\Omega_R = \frac{\langle 1|\hat{\mu}|2\rangle B_0}{\hbar}$ . Here, the magnetic dipole coupling between adjacent states are equal  $\langle +1|\hat{\mu}|0\rangle B_0 = \langle 0|\hat{\mu}|-1\rangle B_0$  due to the equal energy separation between states.

The equal-Rabi interaction Hamiltonian  $\hat{H}_I$  for the three-level system in the rotating wave approximation (RWA) is shown below as adapted from [10, 11].

$$\hat{H}_I = \hbar \begin{bmatrix} \Delta & \frac{1}{\sqrt{2}}\Omega_R e^{-i\phi} & 0 \\ \frac{1}{\sqrt{2}}\Omega_R e^{i\phi} & 0 & \frac{1}{\sqrt{2}}\Omega_R e^{-i\phi} \\ 0 & \frac{1}{\sqrt{2}}\Omega_R e^{i\phi} & -\Delta \end{bmatrix}. \quad (1)$$

Using standard means of solving the eigenvector/eigenvalue problem we find the eigenvalues  $\lambda_i$  via  $|\hat{H}_I - \lambda I|_{det} = 0$  and the eigenvectors  $V_i$  via  $(\hat{H}_I - \lambda I)\vec{V} = 0$  where  $I$  is the identity matrix, leading to

$$[V_1]_{\lambda_1} = \begin{bmatrix} \frac{-\Omega_R}{\sqrt{2}\Omega_G} \\ \frac{\Delta}{\Omega_G} \\ \frac{\Omega_R}{\sqrt{2}\Omega_G} \end{bmatrix}_0, [V_2]_{\lambda_2} = \begin{bmatrix} \frac{1}{2} \left( -1 + \frac{\Delta}{\Omega_G} \right) \\ \frac{\Omega_R}{\sqrt{2}\Omega_G} \\ \frac{1}{2} \left( -1 - \frac{\Delta}{\Omega_G} \right) \end{bmatrix}_{-\hbar\Omega_G}, [V_3]_{\lambda_3} = \begin{bmatrix} \frac{1}{2} \left( 1 + \frac{\Delta}{\Omega_G} \right) \\ \frac{\Omega_R}{\sqrt{2}\Omega_G} \\ \frac{1}{2} \left( 1 - \frac{\Delta}{\Omega_G} \right) \end{bmatrix}_{\hbar\Omega_G}, \quad (2)$$

where  $V_i$  is the eigenvector normalized to 1, the eigenvalues are  $[\lambda_1 \ \lambda_2 \ \lambda_3]^T = [0 \ -\hbar\Omega_G \ \hbar\Omega_G]^T$  and  $\Omega_G = \sqrt{\Delta^2 + \Omega_R^2}$  is the general Rabi frequency.

Once the eigenvalues and eigenvectors are obtained, the unitary time evolution operator  $\hat{U}$  for the general case is  $\hat{U} = \sum_{i=1}^n e^{-\frac{i\lambda_i t}{\hbar}} |V_i\rangle \langle V_i|$ . This expression is derived as  $\hat{H}$  is independent of time in the RWA. However, via the unitary time evolution operator  $\hat{U}$ , we can use  $|\Psi(t)\rangle = \hat{U} |\Psi(0)\rangle$  where  $\hat{U} = e^{\frac{i\hat{H}t}{\hbar}}$  which facilitates an easier method to obtain analytical solutions. Therefore it is crucial to obtain an expression for  $e^{\frac{i\hat{H}t}{\hbar}}$ . In

order to find an expression for  $e^{\frac{i\hat{H}t}{\hbar}}$  we use  $e^x = \sum_{n=0}^{\infty} \frac{x^n}{n!}$  as follows

$$\begin{aligned}
 e^{\frac{i\hat{H}t}{\hbar}} &= \sum_{n=0}^{\infty} \frac{\left(\frac{i\hat{H}t}{\hbar}\right)^n}{n!} \\
 \sum_{k=1}^N e^{\frac{i\hat{H}t}{\hbar}} |V_k\rangle \langle V_k| &= \sum_{k=1}^N \sum_{n=1}^{\infty} \frac{\left(\frac{i\hat{H}t}{\hbar}\right)^n}{n!} |V_k\rangle \langle V_k| \\
 &= \sum_{k=1}^N \sum_{n=1}^{\infty} \frac{\left(\frac{i\lambda_k t}{\hbar}\right)^n}{n!} |V_k\rangle \langle V_k| \quad \text{as } \hat{H}^n |V_k\rangle = \lambda_k^n |V_k\rangle \\
 \hat{U} = e^{\frac{i\hat{H}t}{\hbar}} &= \sum_{k=1}^N e^{\frac{i\lambda_k t}{\hbar}} |V_k\rangle \langle V_k|
 \end{aligned} \tag{3}$$

where  $\lambda_k$  are eigenvalues and  $V_k$  are eigenvectors of  $\hat{H}$ .

The unitary time evolution operator  $\hat{U}$  for the three-level system takes the form

$$\hat{U} = \begin{bmatrix} a_{11} & a_{12} & a_{13} \\ a_{12} & a_{22} & -a_{12}^* \\ a_{13} & -a_{12}^* & a_{11}^* \end{bmatrix}, \tag{4}$$

where the matrix elements  $a_{ij}$  are functions of parameters  $\Delta, \Omega_R, \Omega_G$  and time which takes the form

$$\begin{aligned}
 a_{11} &= \frac{(\Delta^2 + \Omega_G^2) \cos(\Omega_G t) - 2i\Delta\Omega_G \sin(\Omega_G t) + \Omega_R^2}{2\Omega_G^2} \\
 a_{12} &= \frac{\Omega_R (\Delta (\cos(\Omega_G t) - 1) - i\Omega_G \sin(\Omega_G t))}{\sqrt{2}\Omega_G^2} \\
 a_{13} &= \frac{\Omega_R^2 (\cos(\Omega_G t) - 1)}{2\Omega_G^2} \\
 a_{22} &= \frac{\Delta^2 + \Omega_R^2 \cos(\Omega_G t)}{\Omega_G^2}
 \end{aligned} \tag{5}$$

In the case of initially populated top state  $\begin{bmatrix} 1 & 0 & 0 \end{bmatrix}^T$ , the population at the end of the Rabi pulse is shown in Equation 6. In a similar way to the two-level case we find the three-level state vector at any time of the atom-EM interaction  $|\Psi(t)\rangle = \hat{U} |\Psi(0)\rangle$  and the population of each level is

$$P = \begin{bmatrix} |\Psi_{|+1\rangle}|^2 \\ |\Psi_{|0\rangle}|^2 \\ |\Psi_{|-1\rangle}|^2 \end{bmatrix} = \begin{bmatrix} \frac{\Delta^4 + 6\Delta^2\Omega_G^2 + 4\Omega_R^2(\Delta^2 + \Omega_G^2) \cos(\Omega_G t) + (\Delta^2 - \Omega_G^2)^2 \cos(2\Omega_G t) + \Omega_G^4 + 2\Omega_R^4}{8\Omega_G^4} \\ \frac{\Omega_R^2 (\Delta^2 (\cos(\Omega_G t) - 1)^2 + \Omega_G^2 \sin^2(\Omega_G t))}{2\Omega_G^4} \\ \frac{\Omega_R^4 (1 - \cos(\Omega_G t))^2}{4\Omega_G^4} \end{bmatrix} \tag{6}$$

Figure 1 shows the population variation in a three-level system for three combinations of  $\Omega_R$  and  $\Delta$  during the Rabi pulse. The figure shows three interesting

scenarios when the detuning  $\Delta = 0$ ,  $\Delta = \Omega_R$  and  $\Delta = \sqrt{2}\Omega_R$ . The key feature when  $\Delta = \Omega_R$  is that  $|\Psi_{|+1\rangle}|^2 = |\Psi_{|-1\rangle}|^2$  at  $t = \frac{2.221}{\Omega_R}$ . Further, when the detuning increases to  $\Delta = \sqrt{2}\Omega_R$ ,  $|\Psi_{|+1\rangle}|^2 = |\Psi_{|0\rangle}|^2$  at  $t = \frac{1.814}{\Omega_R}$ . Knowledge of these conditions is of great importance as it will assist in improving the stability of the splitting in a three-level Ramsey interferometer such as the  $^{87}\text{Rb}$   $5^2S_{\frac{1}{2}}F = 1$  amidst experimental uncertainties in the applied EM field.

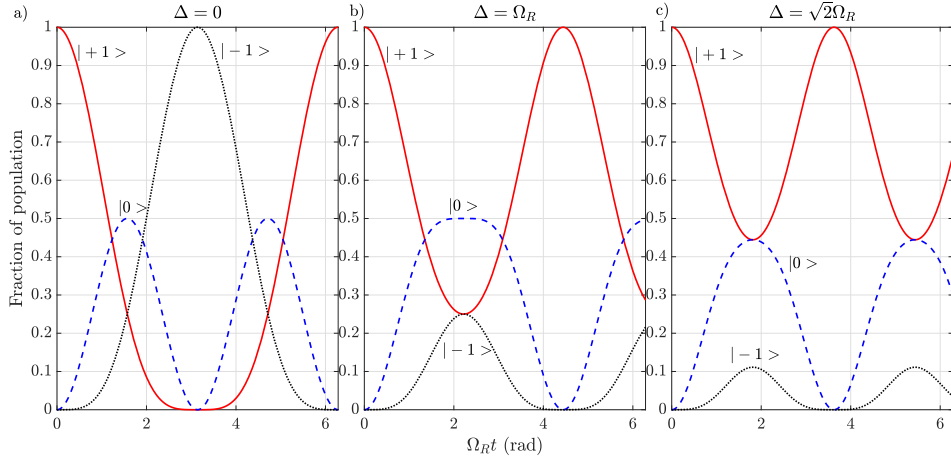


**Figure 1.** Population during the Rabi pulse in a three-level system for three combinations of  $\Omega_R$  and  $\Delta$  where the red solid, blue dashed and black dotted lines denote the populations of states  $|+1\rangle$ ,  $|0\rangle$  and  $|-1\rangle$ , respectively. Detuning are **a)**  $\Delta = 0$ , **b)**  $\Delta = \Omega_R$  and **c)**  $\Delta = \sqrt{2}\Omega_R$ .

For preliminary analysis the equal splitting of  $|\Psi_{|+1\rangle}|^2 = |\Psi_{|0\rangle}|^2$  at the  $\Delta = 0$  condition is explored via the expressions in Equation 6 as the expected Ramsey signal for  $\Delta = 0$  is non-oscillatory. When the equation  $|\Psi_{|+1\rangle}|^2 - |\Psi_{|0\rangle}|^2 = 0$  for  $\Delta = 0$  where  $\Omega_G = \Omega_R$  is simplified the expression  $\frac{1}{8}(4 \cos(\Omega_R t) + 3 \cos(2\Omega_R t) + 1) = 0$  is achieved. When this is solved for  $t$ ,  $t = \frac{\arccos(\frac{1}{3} + 2\pi c_1)}{\Omega_R}$ , where  $c_1$  is an integer and set at  $c_1 = 0$  for the first equal splitting time where  $t = \frac{\arccos(\frac{1}{3})}{\Omega_R}$ . The general unitary time evolution operator  $\hat{U}$  in Equation 4 for the conditions  $\Delta = 0$  and  $t = \frac{\arccos(\frac{1}{3})}{\Omega_R}$  can be substituted leading to the much more simplified form of  $\hat{U}_{\Delta=0}^{Split}$  shown below. Also, the free evolution operator  $\hat{U}_{\Delta=0}^{Free}$  is achieved by substituting  $\Omega_R = \Omega_G = \Delta = 0$  to Equation 4.

$$\hat{U}_{\Delta=0}^{Split} = \begin{bmatrix} \frac{2}{3} & -\frac{2i}{3} & -\frac{1}{3} \\ -\frac{2i}{3} & \frac{1}{3} & -\frac{2i}{3} \\ -\frac{1}{3} & -\frac{2i}{3} & \frac{2}{3} \end{bmatrix}, \quad \hat{U}_{\Delta=0}^{Free} = \begin{bmatrix} 1 & 0 & 0 \\ 0 & 1 & 0 \\ 0 & 0 & 1 \end{bmatrix}. \quad (7)$$

By applying these unitary time evolution operations for each step of the Ramsey sequence, the wavefunction for the three-level system at the end of the sequence takes the form

$$|\Psi_{sys}(t)\rangle = \hat{U}^{Split} \cdot \hat{U}^{Free} \cdot \hat{U}^{Split} \cdot |\Psi(0)\rangle. \quad (8)$$

The resulting system wavefunction  $|\Psi_{sys}(t)\rangle$  is shown below for the starting condition of  $|\Psi(0)\rangle = F = \begin{bmatrix} 1 & 0 & 0 \end{bmatrix}^T$ . This can be easily converted to population which takes the form  $P_{Rsy}$  as

$$|\Psi_{sys}(t)\rangle = \begin{bmatrix} \frac{1}{9} \\ \frac{-4}{9}i \\ \frac{-8}{9} \end{bmatrix}, \quad P_{Rsy} = \begin{bmatrix} \frac{1}{81} \\ \frac{16}{81} \\ \frac{64}{81} \end{bmatrix}, \quad (9)$$

where  $|\Psi_{sys}(t)\rangle$  and  $P_{Rsy}$  are respectively the wavefunction and the population for the three-level system at the end of the Ramsey sequence. Here, the populations of states are at constant values of  $P_{Rsy} = \begin{bmatrix} \frac{1}{81} & \frac{16}{81} & \frac{64}{81} \end{bmatrix}^T$ . The Ramsey signal can be obtained via the average spin projection for a multilevel system  $\langle \hat{F}_Z \rangle = \hbar \sum_{m_F} m_F P_{m_F}$  where  $P_{m_F}$  is the fractional population of the relevant  $m_F$  state [10]. This leads to the constant value of  $\frac{\langle \hat{F}_Z \rangle}{\hbar} = \frac{-7}{9}$  which is the expected behaviour of the system at  $\Delta = 0$ .

The scenario in Figure 1 c) is explored next as the Ramsey signal for  $\Delta \neq 0$  is oscillatory and the equal splitting condition of  $|\Psi_{|+1\rangle}|^2 = |\Psi_{|0\rangle}|^2$  at  $\Delta = \sqrt{2}\Omega_R$  is considered. When the condition  $|\Psi_{|+1\rangle}|^2 - |\Psi_{|0\rangle}|^2 = 0$  for  $\Delta = \sqrt{2}\Omega_R$  where  $\Omega_G = \sqrt{3}\Omega_R$  is applied to Equation 6, the expression  $\frac{1}{6} \cos^2(\frac{1}{2}\sqrt{3}\Omega_R t) (\cos(\sqrt{3}\Omega_R t) + 5) = 0$  is achieved. When this is solved for  $t$ ,  $t = \frac{4\pi c_1 + \pi}{\sqrt{3}\Omega_R}$  where  $c_1$  is an integer and set at  $c_1 = 0$  for the first equal splitting time where  $t = \frac{\pi}{\sqrt{3}\Omega_R}$ . The general unitary time evolution operator  $\hat{U}$  in Equation 4 for the conditions  $\Delta = \sqrt{2}\Omega_R$ ,  $\Omega_G = \sqrt{3}\Omega_R$  and  $t = \frac{\pi}{\sqrt{3}\Omega_R}$  can be substituted and takes the much more simplified form of  $\hat{U}_{\Delta=\sqrt{2}\Omega_R}^{Split}$  shown in Equation 10. Further, the operator during free evolution is derived from Equations 4 via Equations 5 for the conditions  $\Omega_R = 0$  when the general Rabi frequency  $\Omega_G = \Delta$  for an evolution time  $t = T$ . This leads to the free evolution operator  $\hat{U}_{\Omega_R=0}^{Free}$  in Equation 10,

$$\hat{U}_{\Delta=\sqrt{2}\Omega_R}^{Split} = \begin{bmatrix} -\frac{2}{3} & -\frac{2}{3} & -\frac{1}{3} \\ -\frac{2}{3} & \frac{1}{3} & \frac{2}{3} \\ -\frac{1}{3} & \frac{2}{3} & -\frac{2}{3} \end{bmatrix}, \quad \hat{U}_{\Omega_R=0}^{Free} = \begin{bmatrix} e^{-iT\Delta} & 0 & 0 \\ 0 & 1 & 0 \\ 0 & 0 & e^{iT\Delta} \end{bmatrix}. \quad (10)$$

Following Equation 8 for the full sequence, the wavefunction for the three-level system at the end of the Ramsey sequence takes the form for the condition of  $\Delta = \sqrt{2}\Omega_R$

$$|\Psi_{sys}(T)\rangle = \begin{bmatrix} \frac{1}{9}(5 \cos(\Delta T) - 3i \sin(\Delta T) + 4) \\ \frac{2}{9}(\cos(\Delta T) - 3i \sin(\Delta T) - 1) \\ \frac{4}{9}(\cos(\Delta T) - 1) \end{bmatrix}, \quad (11)$$

Further, an overall expression for the Ramsey signal can be obtained when the average spin projection for a multilevel system  $\langle \hat{F}_Z \rangle = \hbar \sum_{m_F} m_F P_{m_F}$  is applied. Based on  $\langle \hat{F}_Z \rangle$  the Ramsey signal takes the form  $\frac{\langle \hat{F}_Z \rangle}{\hbar} = \frac{1}{9}(1 + 8 \cos(\Delta T))$  where the Ramsey signal and populations of each state are shown in Figure 2.



precursor for the five-level Rabi signal, [10] via [18, 11], shows that the analytical solutions for the transition probabilities of a spin- $F$  system with  $2F + 1$  sub-levels can be obtained via expressions for  $C_1(t)$  and  $C_2(t)$  in Equation ?? for the two-level system as below;

$$\Psi_{m_F} = \sqrt{\frac{(2F)!}{(F+m_F)!(F-m_F)!}} C_1(t)^{F-m_F} C_2(t)^{F+m_F} \quad m_F \in \{-F \rightarrow F\}$$

$$\begin{aligned} |\Psi_{|-2\rangle}|^2 &= (|C_1|^2)^4, \\ |\Psi_{|-1\rangle}|^2 &= 4(|C_1|^2)^3(1 - |C_1|^2), \\ |\Psi_{|0\rangle}|^2 &= 6(|C_1|^2)^2(1 - |C_1|^2)^2, \\ |\Psi_{|+1\rangle}|^2 &= 4(|C_1|^2)(1 - |C_1|^2)^3, \\ |\Psi_{|+2\rangle}|^2 &= (1 - |C_1|^2)^4, \end{aligned} \quad (12)$$

where  $C_1(t), C_2(t)$  are defined in Equation ?? and  $|C_1|^2 = |C_1(t)|^2 = \frac{\Omega_R^2}{\Omega_G^2} \sin^2(\frac{\Omega_G t}{2})$ .

Based on this approach, the evolution of the fractional population of each level when the BEC starts in  $|+2\rangle$  can be derived as shown in Equation 12. It should be noted that this treatment can be applied to arbitrary values of  $F$  and is only valid for linearly shifted Zeeman levels coupled via magnetic dipole transitions. Figure 4 **a**) presents the on-resonance ( $\Delta = 0$ ) analytical solutions for Equation 12 [10] showing the fractional population of each level with respect to the Rabi pulse area. The red line denotes the population variation of the state  $|+2\rangle$  and the blue line of the state  $|+1\rangle$ . The analytical solution shows that the two levels create an equal population fraction of 0.41 at  $\sin(\frac{\Omega_R t}{2}) = \frac{1}{\sqrt{5}}$ , where  $\frac{\Omega_R t}{2} = 0.46 \text{ rad}$  or  $2.68 \text{ rad}$ . At this time 18% of the atoms from the total cloud are in the  $|0\rangle$  and  $|-1\rangle$  states. This is reflected in Figure 4 **b**) which represents the fraction of atom numbers in state  $|+1\rangle$  and  $|+2\rangle$  with respect to the combined  $|+1\rangle - |+2\rangle$  system. The red solid line with circles is the fractional population of  $|+2\rangle$  and the blue solid line with squares is the fractional population of  $|+1\rangle$ . The black dashed line shows the dynamics of the combined  $|+1\rangle - |+2\rangle$  system where the atoms move to other states of the five-level system. Figure 4 **b**) indicates that any population mix where  $|+2\rangle \in \{100\% \rightarrow 50\%\}$  and  $|+1\rangle \in \{0\% \rightarrow 50\%\}$  is possible with minimal loss of atoms in the range  $\frac{\Omega_R t}{2} \in \{0 \text{ rad} \rightarrow 0.46 \text{ rad}\}$ . However, going beyond this point the superposition leads to a fast decay of the signal where the atoms quickly move out of the desired  $|+1\rangle - |+2\rangle$  states which recovers back when  $\frac{\Omega_R t}{2} = 2.68 \text{ rad}$ . Between  $\frac{\Omega_R t}{2} \in \{2.68 \text{ rad} \rightarrow 3.14 \text{ rad}\}$  the other half of the combination of superpositions from  $|+2\rangle \in \{50\% \rightarrow 100\%\}$  and  $|+1\rangle \in \{50\% \rightarrow 0\%\}$  are available.

We will use the interaction Hamiltonian  $\hat{H}_I$  for a five-level system in the form of Equation 13 which takes into account the Clebsch-Gordon coefficients for the



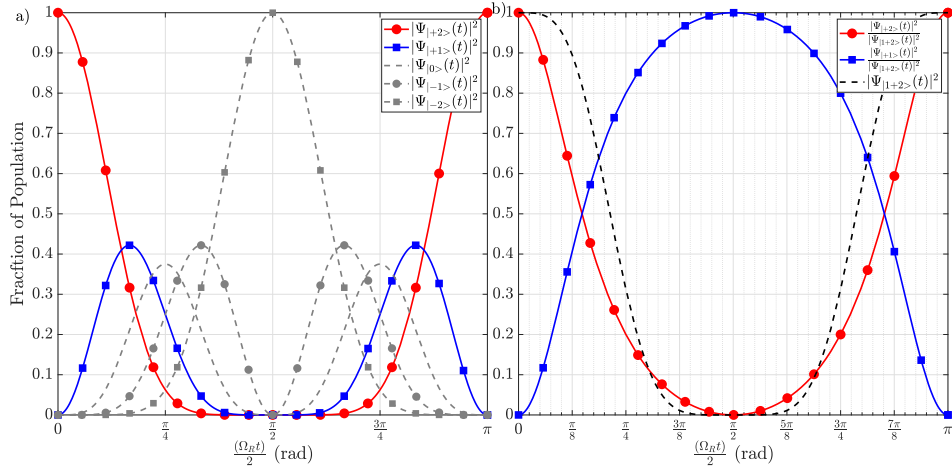


**Figure 4.** Resonant Rabi oscillations in the  $F = 2$  system according to Equation 12. **a)** Evolution of populations of the five states with time, **b)** population fraction in state  $|+1\rangle$  (blue solid line with squares) and in state  $|+2\rangle$  (red solid line with circles) relative to the combined population of the two states  $|+1\rangle$  and  $|+2\rangle$ . The black dashed line shows the combined population of states  $|+1\rangle - |+2\rangle$ .

corresponding  $F = 2$  hyperfine manifold [10].

$$\hat{H}_I = \hbar \begin{bmatrix} 2\Delta & \Omega_R & 0 & 0 & 0 \\ \Omega_R & \Delta & \sqrt{\frac{3}{2}}\Omega_R & 0 & 0 \\ 0 & \sqrt{\frac{3}{2}}\Omega_R & 0 & \sqrt{\frac{3}{2}}\Omega_R & 0 \\ 0 & 0 & \sqrt{\frac{3}{2}}\Omega_R & -\Delta & \Omega_R \\ 0 & 0 & 0 & \Omega_R & -2\Delta \end{bmatrix} \quad (13)$$

where  $\hbar$  is the reduced Planck's constant,  $\Delta$  is the detuning of the external laser field from the energy separation between adjacent states and  $\Omega_R = \frac{\mu_0 g_F B_\perp}{\hbar}$  [10] is the resonant Rabi frequency.

Again, using the standard method of solving the eigenvalue-eigenvector problem we solve for the normalised eigenvalues  $\lambda_i$  and the eigenvectors  $V_i$ . Once the eigenvalues and eigenvectors are obtained, the unitary time evolution operator  $\hat{U}$  for the general case is found via  $\hat{U} = \sum_{i=1}^n e^{\frac{-i\lambda_i t}{\hbar}} |V_i\rangle \langle V_i|$ . The resulting bare matrix is sizeable beyond several pages. To simplify, the relation of  $\Delta = \alpha\Omega_R$  (leading to  $\alpha = \frac{\Delta}{\Omega_R}$ ) is introduced where  $\Omega_G = \sqrt{1 + \alpha^2}\Omega_R$ . With this the evolution operator  $\hat{U}$  takes the reduced form of

$$\hat{U} = \begin{bmatrix} a_{11} & a_{12} & a_{13} & a_{14} & a_{15} \\ a_{12} & a_{22} & a_{23} & a_{24} & -a_{14}^* \\ a_{13} & a_{23} & a_{33} & -a_{23}^* & a_{13}^* \\ a_{14} & a_{24} & -a_{23}^* & a_{22}^* & -a_{12}^* \\ a_{15} & -a_{14}^* & a_{13}^* & -a_{12}^* & a_{11}^* \end{bmatrix}, \quad (14)$$

where  $a_{ij}^*$  is the complex conjugate and  $a_{ij} = f(\alpha, \Omega_R, t)$  which take the following form;

$$\begin{aligned}
 a_{11} &= \frac{(8\alpha^2+4)\cos(\Omega_G t) - 8i\alpha\sqrt{\alpha^2+1}\sin(\Omega_G t)\left(\left(2\alpha^2+1\right)\cos(\Omega_G t)+1\right) + \left(8(\alpha^4+\alpha^2)+1\right)\cos(2\Omega_G t)+3}{8(\alpha^2+1)^2} \\
 a_{12} &= \frac{(4\alpha^2+3)\alpha\cos(2\Omega_G t) + i(-2\sqrt{\alpha^2+1}\sin(\Omega_G t)\left(-2\alpha^2+(4\alpha^2+1)\cos(\Omega_G t)+1\right) + 3i\alpha) - 4\alpha^3\cos(\Omega_G t)}{4(\alpha^2+1)^2} \\
 a_{13} &= -\frac{\sqrt{\frac{3}{2}}\sin^2\left(\frac{1}{2}\Omega_G t\right)\left(-2i\alpha\sqrt{\alpha^2+1}\sin(\Omega_G t) + (2\alpha^2+1)\cos(\Omega_G t)+1\right)}{(\alpha^2+1)^2} \\
 a_{14} &= \frac{2\sin^3\left(\frac{1}{2}\Omega_G t\right)\left(\alpha\sin\left(\frac{1}{2}\Omega_G t\right) + i\sqrt{\alpha^2+1}\cos\left(\frac{1}{2}\Omega_G t\right)\right)}{(\alpha^2+1)^2} \\
 a_{15} &= \frac{\sin^4\left(\frac{1}{2}\Omega_G t\right)}{(\alpha^2+1)^2} \\
 a_{22} &= \frac{(\alpha^2+2\cos(\Omega_G t)-1)\left(-2i\alpha\sqrt{\alpha^2+1}\sin(\Omega_G t) + (2\alpha^2+1)\cos(\Omega_G t)+1\right)}{2(\alpha^2+1)^2} \\
 a_{23} &= -\frac{\sqrt{6}\sin\left(\frac{1}{2}\Omega_G t\right)\left(\alpha^2+\cos(\Omega_G t)\right)\left(\alpha\sin\left(\frac{1}{2}\Omega_G t\right) + i\sqrt{\alpha^2+1}\cos\left(\frac{1}{2}\Omega_G t\right)\right)}{(\alpha^2+1)^2} \\
 a_{24} &= -\frac{\sin^2\left(\frac{1}{2}\Omega_G t\right)\left(3\alpha^2+2\cos(\Omega_G t)+1\right)}{(\alpha^2+1)^2} \\
 a_{33} &= \frac{(1-2\alpha^2)^2 + 12\alpha^2\cos(\Omega_G t) + 3\cos(2\Omega_G t)}{4(\alpha^2+1)^2}
 \end{aligned} \tag{15}$$

The population at the end of the Rabi pulse can be obtained when this  $\hat{U}$  is applied to the starting state of  $|+2\rangle$   $F = \begin{bmatrix} 0 & 0 & 0 & 0 & 1 \end{bmatrix}^T$  where the population at the end of the pulse is

$$P = \begin{bmatrix} |\Psi_{|-2\rangle}|^2 \\ |\Psi_{|-1\rangle}|^2 \\ |\Psi_{|0\rangle}|^2 \\ |\Psi_{|+1\rangle}|^2 \\ |\Psi_{|+2\rangle}|^2 \end{bmatrix} = \begin{bmatrix} \frac{\sin^8\left(\frac{1}{2}\Omega_G t\right)}{(\alpha^2+1)^4} \\ \frac{2(2\alpha^2+\cos(\Omega_G t)+1)\sin^6\left(\frac{1}{2}\Omega_G t\right)}{(\alpha^2+1)^4} \\ \frac{3(2\alpha^2+\cos(\Omega_G t)+1)^2\sin^4\left(\frac{1}{2}\Omega_G t\right)}{2(\alpha^2+1)^4} \\ \frac{(2\alpha^2+\cos(\Omega_G t)+1)^3\sin^2\left(\frac{1}{2}\Omega_G t\right)}{2(\alpha^2+1)^4} \\ \frac{(2\alpha^2+\cos(\Omega_G t)+1)^4}{16(\alpha^2+1)^4} \end{bmatrix} \tag{16}$$

where  $\Delta = \alpha\Omega_R$  and  $\Omega_G = \sqrt{1+\alpha^2}\Omega_R$ .

When the equal splitting condition is applied where  $|\Psi_{|+2\rangle}|^2 = |\Psi_{|+1\rangle}|^2$  and solved for  $t$ , the equal splitting occurs at  $t = \frac{4\left(\tan^{-1}\left(\sqrt{\frac{-\alpha^2+2\sqrt{5}\sqrt{4-\alpha^2+9}}{\alpha^2+1}}\right) + \pi c_1\right)}{\Omega_G}$  where  $c_1$  is an integer. The first equal splitting occurs at  $c_1 = 0$  where  $t_{Split} = \frac{4\tan^{-1}\left(\sqrt{\frac{-\alpha^2+2\sqrt{5}\sqrt{4-\alpha^2+9}}{\alpha^2+1}}\right)}{\Omega_G}$ . When this condition is applied to  $\hat{U}$  in Equation 14, the splitting matrix takes the form

$$\hat{U}_G^{Split} = \begin{bmatrix} A_{11} & A_{12} & A_{13} & A_{14} & A_{15} \\ A_{12} & A_{22} & A_{23} & A_{24} & -A_{14}^* \\ A_{13} & A_{23} & A_{33} & -A_{23}^* & A_{13}^* \\ A_{14} & A_{24} & -A_{23}^* & A_{22}^* & -A_{12}^* \\ A_{15} & -A_{14}^* & A_{13}^* & -A_{12}^* & A_{11}^* \end{bmatrix}, \hat{U}_{\Omega_R=0}^{Free} = \begin{bmatrix} e^{-2it\Delta} & 0 & 0 & 0 & 0 \\ 0 & e^{-it\Delta} & 0 & 0 & 0 \\ 0 & 0 & 1 & 0 & 0 \\ 0 & 0 & 0 & e^{it\Delta} & 0 \\ 0 & 0 & 0 & 0 & e^{2it\Delta} \end{bmatrix} \tag{17}$$

where  $\hat{U}_G^{Split}$  is achieved by substituting  $t = t_{Split}$  to Equation 14 where the full expressions are where  $A_{ij} = f(\alpha)$  and the full expressions are as follows;

$$\begin{aligned}
 A_{11} &= \frac{4\left(2(\alpha^8 - 2\alpha^6 - 5\alpha^4 + 2) + 5i\alpha(\alpha^2 - 2)(\alpha^2 + 1)^{3/2} \sin(\Omega_G t_{Split})\right)}{25(\alpha^2 + 1)^2} \\
 A_{12} &= \frac{\frac{8}{25} \left( \alpha(\alpha^2 + 1)(\alpha^2 - 3) + 25i \left( -\frac{(\alpha^2 - 1)(\alpha^2 + 1)^{5/2} (\alpha^2 - 2\sqrt{5}\sqrt{4 - \alpha^2} - 9)(\alpha^2 - \sqrt{5}\sqrt{4 - \alpha^2} - 4) \sqrt{\frac{-\alpha^2 + 2\sqrt{5}\sqrt{4 - \alpha^2} + 9}{\alpha^2 + 1}}}{(\sqrt{5}\sqrt{4 - \alpha^2} + 5)^4} \right) \right)}{(\alpha^2 + 1)^2} \\
 A_{13} &= \frac{1}{25} \sqrt{6} \left( 2\alpha^2 + \frac{5i\alpha \sin(\Omega_G t_{Split})}{\sqrt{\alpha^2 + 1}} - 4 \right) \\
 A_{14} &= \frac{2 \sin^3\left(\frac{\Omega_G t_{Split}}{2}\right) \left( \alpha \sin\left(\frac{\Omega_G t_{Split}}{2}\right) + i\sqrt{\alpha^2 + 1} \cos\left(\frac{\Omega_G t_{Split}}{2}\right) \right)}{(\alpha^2 + 1)^2} \\
 A_{15} &= \frac{1}{25} \\
 A_{22} &= \frac{1}{25} \left( -2\alpha^2 - \frac{5i\alpha \sin(\Omega_G t_{Split})}{\sqrt{\alpha^2 + 1}} + 4 \right) \\
 A_{23} &= \frac{3}{25} \sqrt{\frac{3}{2}} \left( -2\alpha - \frac{5i \sin(\Omega_G t_{Split})}{\sqrt{\alpha^2 + 1}} \right) \\
 A_{24} &= -\frac{11}{25} \\
 A_{33} &= \frac{1}{25}
 \end{aligned} \tag{18}$$

One can easily obtain the expression for the system wavefunction at the end of the Ramsey sequence by applying  $\hat{U}_G^{Split}$ ,  $\hat{U}_{\Omega_R=0}^{Free}$  to Equation 8 which then can be converted to populations and Ramsey signal via  $\langle \hat{F}_Z \rangle = \hbar \sum_{m_F} m_F P_{m_F}$ . However, these expressions are omitted due to the immense length. These expressions reduce to a much more convenient form when a specific relation between  $\Delta$  and  $\Omega_R$  via  $\Delta = \alpha\Omega_R$  is applied. Preliminarily, two conditions of  $\Delta = 0$  and  $\Delta = 2\Omega_R$  will be considered. In the first case, when  $\Delta = 0 \rightarrow \Omega_G = \Omega_R$ , which is substituted into  $\hat{U}$  in Equation 14 to obtain

$$\hat{U}_{\Delta=0} = \begin{bmatrix} b_{11} & b_{12} & b_{13} & b_{14} & b_{15} \\ b_{12} & b_{22} & b_{23} & b_{24} & -b_{14}^* \\ b_{13} & b_{23} & b_{33} & -b_{23}^* & b_{13}^* \\ b_{14} & b_{24} & -b_{23}^* & b_{22}^* & -b_{12}^* \\ b_{15} & -b_{14}^* & b_{13}^* & -b_{12}^* & b_{11}^* \end{bmatrix} \tag{19}$$

where  $b_{ij} = f(\Omega_R, t)$  and the full expressions are

$$\begin{aligned}
 b_{11} &= \cos^4\left(\frac{\Omega_R t}{2}\right) & b_{22} &= \frac{1}{2} (\cos(\Omega_R t) + \cos(2\Omega_R t)) \\
 b_{12} &= -\frac{1}{4}i (2 \sin(\Omega_R t) + \sin(2\Omega_R t)) & b_{23} &= -\frac{1}{2}i \sqrt{\frac{3}{2}} \sin(2\Omega_R t) \\
 b_{13} &= -\frac{1}{2} \sqrt{\frac{3}{2}} \sin^2(\Omega_R t) & b_{24} &= \frac{1}{2} (\cos(2\Omega_R t) - \cos(\Omega_R t)) \\
 b_{14} &= i \sin^2\left(\frac{\Omega_R t}{2}\right) \sin(\Omega_R t) & b_{33} &= \frac{1}{4} (3 \cos(2\Omega_R t) + 1) \\
 b_{15} &= \sin^4\left(\frac{\Omega_R t}{2}\right)
 \end{aligned} \tag{20}$$

The population  $P_{\Delta=0}$  at the end of the Rabi pulse for a specific starting state can be obtained by applying  $\hat{U}_{\Delta=0}$  to the starting state. For the case of starting from the

top state  $|+2\rangle$   $F = \begin{bmatrix} 0 & 0 & 0 & 0 & 1 \end{bmatrix}^T$ , the population at the end of the Rabi pulse is

$$P_{\Delta=0} = \begin{bmatrix} |\Psi_{|-2\rangle}|^2 \\ |\Psi_{|-1\rangle}|^2 \\ |\Psi_{|0\rangle}|^2 \\ |\Psi_{|+1\rangle}|^2 \\ |\Psi_{|+2\rangle}|^2 \end{bmatrix} = \begin{bmatrix} \sin^8\left(\frac{\Omega_R t}{2}\right) \\ \sin^4\left(\frac{\Omega_R t}{2}\right) \sin^2(\Omega_R t) \\ \frac{3}{8} \sin^4(\Omega_R t) \\ \frac{1}{16} (2 \sin(\Omega_R t) + \sin(2\Omega_R t))^2 \\ \cos^8\left(\frac{\Omega_R t}{2}\right) \end{bmatrix} \quad (21)$$

These analytical formulae for the population after the Rabi pulse are compared with expressions in Equation 12 based on the two-level formalism as shown in Figure 5. The figure shows an exact overlap validating the expressions derived in Equation 21.

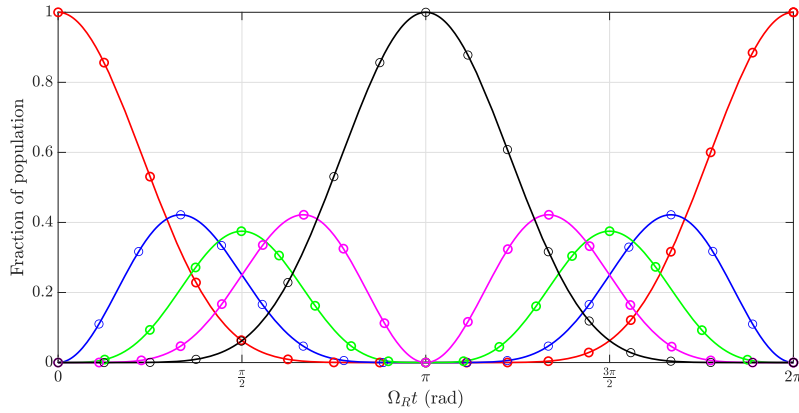


**Figure 5.** Resonant ( $\Delta = 0$ ) Rabi oscillations of populations in the five-level system using the analytical form of Equation 21 (solid lines) and of the  $C_1, C_2$  representation of Equation 12 (open circles). Colours for states follow red -  $|+2\rangle$ , blue -  $|+1\rangle$ , green -  $|0\rangle$ , magenta -  $|-1\rangle$  and black -  $|-2\rangle$ .

As shown above, during resonant Rabi interactions the atoms starting in state  $|+2\rangle$  leave the state and occupy state  $|+1\rangle$ . As the EM pulse continues, this effect pushes atoms towards state  $|-2\rangle$  via states  $|0\rangle$  and  $|-1\rangle$ . Due to resonance, all atoms occupy  $|-2\rangle$  and the system undergoes full inversion after which the atoms recover back to the initial state  $|+2\rangle$  and continue to produce Rabi oscillations.

Moving on, the speciality of  $\Delta = 2\Omega_R$  is that the two states of interest  $|+1\rangle$  and  $|+2\rangle$  do not cross when  $\Delta$  increases beyond this point eliminating the possibility of creating a superposition with equal splitting. When  $\Delta = 2\Omega_R \rightarrow \Omega_G = \sqrt{5}\Omega_R$  is substituted into  $\hat{U}$  in Equation 14 the  $\hat{U}_{\Delta=2\Omega_R}$  we obtain

$$\hat{U} = \begin{bmatrix} c_{11} & c_{12} & c_{13} & c_{14} & c_{15} \\ c_{12} & c_{22} & c_{23} & c_{24} & -c_{14}^* \\ c_{13} & c_{23} & c_{33} & -c_{23}^* & c_{13}^* \\ c_{14} & c_{24} & -c_{23}^* & c_{22}^* & -c_{12}^* \\ c_{15} & -c_{14}^* & c_{13}^* & -c_{12}^* & c_{11}^* \end{bmatrix}, \quad (22)$$

where  $c_{ij} = f(\Omega_R, t)$  and the full expressions are

$$\begin{aligned}
 c_{11} &= \frac{1}{200} \left( -16i\sqrt{5} \sin(\sqrt{5}\Omega_R t) - 72i\sqrt{5} \sin(2\sqrt{5}\Omega_R t) + 36 \cos(\sqrt{5}\Omega_R t) + 161 \cos(2\sqrt{5}\Omega_R t) + 3 \right) \\
 c_{12} &= \frac{1}{100} \left( -17i\sqrt{5} \sin(2\sqrt{5}\Omega_R t) + 14i\sqrt{5} \sin(\sqrt{5}\Omega_R t) - 32 \cos(\sqrt{5}\Omega_R t) + 38 \cos(2\sqrt{5}\Omega_R t) - 6 \right) \\
 c_{13} &= \frac{1}{25} \sqrt{\frac{3}{2}} \sin^2\left(\frac{1}{2}\sqrt{5}\Omega_R t\right) \left( 4i\sqrt{5} \sin(\sqrt{5}\Omega_R t) - 9 \cos(\sqrt{5}\Omega_R t) - 1 \right) \\
 c_{14} &= \frac{2}{25} \sin^3\left(\frac{1}{2}\sqrt{5}\Omega_R t\right) \left( 2 \sin\left(\frac{1}{2}\sqrt{5}\Omega_R t\right) + i\sqrt{5} \cos\left(\frac{1}{2}\sqrt{5}\Omega_R t\right) \right) \\
 c_{15} &= \frac{1}{25} \sin^4\left(\frac{1}{2}\sqrt{5}\Omega_R t\right) \\
 c_{22} &= \frac{1}{50} \left( 2 \cos(\sqrt{5}\Omega_R t) + 3 \right) \left( -4i\sqrt{5} \sin(\sqrt{5}\Omega_R t) + 9 \cos(\sqrt{5}\Omega_R t) + 1 \right) \\
 c_{23} &= \frac{1}{50} \sqrt{\frac{3}{2}} \left( -8i\sqrt{5} \sin(\sqrt{5}\Omega_R t) - i\sqrt{5} \sin(2\sqrt{5}\Omega_R t) + 12 \cos(\sqrt{5}\Omega_R t) + 2 \cos(2\sqrt{5}\Omega_R t) - 14 \right) \\
 c_{24} &= \frac{1}{50} \left( 11 \cos(\sqrt{5}\Omega_R t) + \cos(2\sqrt{5}\Omega_R t) - 12 \right) \\
 c_{33} &= \frac{1}{100} \left( 48 \cos(\sqrt{5}\Omega_R t) + 3 \cos(2\sqrt{5}\Omega_R t) + 49 \right)
 \end{aligned} \tag{23}$$

The population  $P_{\Delta=2\Omega_R}$  at the end of the Rabi pulse for a specific starting state can be obtained by applying  $\hat{U}_{\Delta=2\Omega_R}$  to the starting state. For the case of starting from the top state when  $F = \begin{bmatrix} 0 & 0 & 0 & 0 & 1 \end{bmatrix}^T$ , the population at the end of the Rabi pulse is

$$P_{\Delta=2\Omega_R} = \begin{bmatrix} |\Psi_{|-2\rangle}|^2 \\ |\Psi_{|-1\rangle}|^2 \\ |\Psi_{|0\rangle}|^2 \\ |\Psi_{|+1\rangle}|^2 \\ |\Psi_{|+2\rangle}|^2 \end{bmatrix} = \begin{bmatrix} \frac{1}{625} \sin^8\left(\frac{1}{2}\sqrt{5}\Omega_R t\right) \\ \frac{2}{625} \sin^6\left(\frac{1}{2}\sqrt{5}\Omega_R t\right) (\cos(\sqrt{5}\Omega_R t) + 9) \\ \frac{3 \sin^4\left(\frac{1}{2}\sqrt{5}\Omega_R t\right) (\cos(\sqrt{5}\Omega_R t) + 9)^2}{1250} \\ \frac{\sin^2\left(\frac{1}{2}\sqrt{5}\Omega_R t\right) (\cos(\sqrt{5}\Omega_R t) + 9)^3}{1250} \\ \frac{(\cos(\sqrt{5}\Omega_R t) + 9)^4}{10000} \end{bmatrix} \tag{24}$$

Rabi oscillations of the populations show non-resonant behaviour when the initially populated state  $|+2\rangle$  exhibits variations in the range 1 - 0.41 and state  $|+1\rangle$  in the range 0 - 0.41 as shown in Figure 6. All other states show significantly smaller variations.

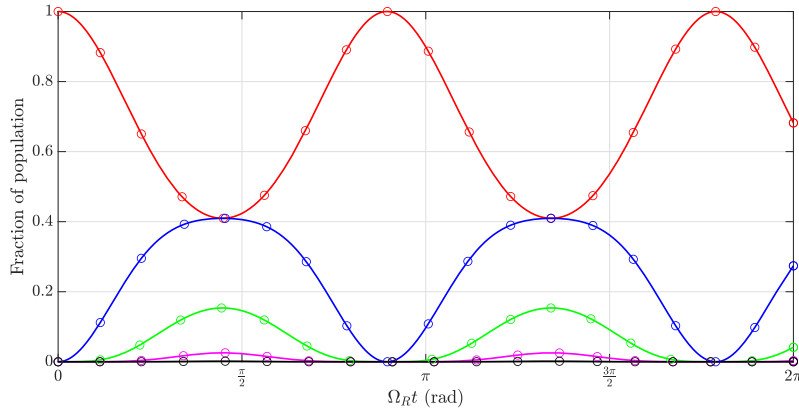


**Figure 6.** Non-resonant ( $\Delta = 2\Omega_R$ ) Rabi oscillations of populations in the five-level system using the analytical form of Equation 24 (solid lines) and of the  $C_1, C_2$  presentation of Equation 12 (open circles). Colours for states follow red -  $|+2\rangle$ , blue -  $|+1\rangle$ , green -  $|0\rangle$ , magenta -  $|-1\rangle$  and black -  $|-2\rangle$ .

### 3.2. Ramsey signal for the two interesting cases

Firstly, for the resonant case where  $\Delta = 0$ , we are interested in the equal splitting of states  $|+2\rangle$  and  $|+1\rangle$ . The equal population condition is applied between states  $|+2\rangle$  and  $|+1\rangle$  to obtain an expression for the pulse duration. When  $|\Psi_{|+2\rangle}|^2 = |\Psi_{|+1\rangle}|^2$  is applied to Equation 21,  $-\frac{1}{4}\sin^2(\Omega_R t) - \frac{1}{16}\sin^2(2\Omega_R t) - \frac{1}{4}\sin(\Omega_R t)\sin(2\Omega_R t) + \cos^8\left(\frac{\Omega_R t}{2}\right) = 0$  is achieved where the acceptable terms for  $t$  take the form  $t = \frac{4(\pi c_1 + \tan^{-1}(2+\sqrt{5}))}{\Omega_R}$  or  $t = -\frac{4(\pi c_1 + \tan^{-1}(2-\sqrt{5}))}{\Omega_R}$ , where  $c_1$  is an integer. The first equal splitting occurs at  $c_1 = 0$  where  $t = -\frac{4(\tan^{-1}(2-\sqrt{5}))}{\Omega_R}$ . When this condition is applied to  $\hat{U}_{\Delta=0}$  in Equation 19 the desired time evolution operator  $\hat{U}_{\Delta=0}^{Split}$  for equal splitting is obtained.

$$\hat{U}_{\Delta=0}^{Split} = \begin{bmatrix} \frac{16}{25} & \frac{16i}{25} & -\frac{4\sqrt{6}}{25} & -\frac{4i}{25} & \frac{1}{25} \\ \frac{16i}{25} & \frac{4}{25} & \frac{6i\sqrt{6}}{25} & -\frac{11}{25} & -\frac{4i}{25} \\ -\frac{4\sqrt{6}}{25} & \frac{6i\sqrt{6}}{25} & \frac{1}{25} & \frac{6i\sqrt{6}}{25} & -\frac{4\sqrt{6}}{25} \\ -\frac{4i}{25} & -\frac{11}{25} & \frac{6i\sqrt{6}}{25} & \frac{4}{25} & \frac{16i}{25} \\ \frac{1}{25} & -\frac{4i}{25} & -\frac{4\sqrt{6}}{25} & \frac{16i}{25} & \frac{16}{25} \end{bmatrix}, \hat{U}_{\Delta=0}^{Free} = \begin{bmatrix} 1 & 0 & 0 & 0 & 0 \\ 0 & 1 & 0 & 0 & 0 \\ 0 & 0 & 1 & 0 & 0 \\ 0 & 0 & 0 & 1 & 0 \\ 0 & 0 & 0 & 0 & 1 \end{bmatrix} \quad (25)$$

where  $\hat{U}_{\Delta=0}^{Split}$  is achieved by substituting  $\Delta = 0, \Omega_G = \Omega_R$  and  $t = -\frac{4(\tan^{-1}(2-\sqrt{5}))}{\Omega_R}$  to Equation 14 and  $\hat{U}_{\Delta=0}^{Free}$  is achieved by extrapolating from Equation 7.

Following on from Equation 7, the time evolution operator during free evolution  $\hat{U}_{\Delta=0}^{Free}$  is the identity matrix as shown in Equation 25. The equation for the system wavefunction at the end of the Ramsey sequence can be obtained by applying Equation 8

$$|\Psi_{sys}(t)\rangle = \begin{bmatrix} \frac{81}{625} \\ \frac{216i}{625} \\ -\frac{144\sqrt{6}}{625} \\ -\frac{384i}{625} \\ \frac{256}{625} \end{bmatrix}, P_{Rsy} = \begin{bmatrix} \frac{65536}{390625} \\ \frac{147456}{390625} \\ \frac{124416}{390625} \\ \frac{46656}{390625} \\ \frac{6561}{390625} \end{bmatrix}, \quad (26)$$

where  $|\Psi_{sys}(t)\rangle$  and  $P_{Rsy}$  are respectively the vector state and the populations for the five-level system at the end of the Ramsey sequence.

This can be easily converted to population which takes the form  $P_{Rsy}$  in Equation 26 which shows constant values for the populations of each state at  $P_{Rsy} = \left[ \frac{65536}{390625} \quad \frac{147456}{390625} \quad \frac{124416}{390625} \quad \frac{46656}{390625} \quad \frac{6561}{390625} \right]^T$ . Further, an overall expression for the Ramsey signal can be obtained when the average spin projection for a multilevel system  $\langle \hat{F}_Z \rangle = \hbar \sum_{m_F} m_F P_{m_F}$  is applied, where  $P_{m_F}$  is the fractional population of the relevant state [10]. This leads to a constant value for the Ramsey signal at  $\frac{\langle \hat{F}_Z \rangle}{\hbar} = \frac{-14}{25}$  which is the expected behaviour of the system.

For the second scenario, the detuning  $\Delta = 2\Omega_R$  was chosen and when equal population condition of  $|\Psi_{|+2\rangle}|^2 = |\Psi_{|+1\rangle}|^2$  is applied to the expressions Equation 24, leads to  $\frac{(\cos(\sqrt{5}\Omega_R t) + 9)^4}{10000} - \frac{\sin^2\left(\frac{1}{2}\sqrt{5}\Omega_R t\right)(\cos(\sqrt{5}\Omega_R t) + 9)^3}{1250} = 0$ . Here, the acceptable term for

$t$  takes the form  $t = \frac{4\pi c_1 + \pi}{\sqrt{5}\Omega_R}$ , where  $c_1$  is an integer. The first equal splitting occurs at  $c_1 = 0$  where  $t = \frac{\pi}{\sqrt{5}\Omega_R}$ . When this condition is applied to  $\hat{U}_{\Delta=2\Omega_R}$  in Equation 22 the desired time evolution operator  $\hat{U}_{\Delta=2\Omega_R}^{Split}$  for equal splitting is obtained.

$$\hat{U}_{\Delta=2\Omega_R}^{Split} = \begin{bmatrix} \frac{16}{25} & \frac{16}{25} & \frac{4\sqrt{6}}{25} & \frac{4}{25} & \frac{1}{25} \\ \frac{16}{25} & -\frac{4}{25} & -\frac{6\sqrt{6}}{25} & -\frac{11}{25} & -\frac{4}{25} \\ \frac{4\sqrt{6}}{25} & -\frac{6\sqrt{6}}{25} & \frac{1}{25} & \frac{6\sqrt{6}}{25} & \frac{4\sqrt{6}}{25} \\ \frac{4}{25} & -\frac{11}{25} & \frac{6\sqrt{6}}{25} & -\frac{4}{25} & -\frac{16}{25} \\ \frac{1}{25} & -\frac{4}{25} & \frac{4\sqrt{6}}{25} & -\frac{16}{25} & \frac{16}{25} \end{bmatrix}, \hat{U}_{\Omega_R=0}^{Free} = \begin{bmatrix} e^{-2it\Delta} & 0 & 0 & 0 & 0 \\ 0 & e^{-it\Delta} & 0 & 0 & 0 \\ 0 & 0 & 1 & 0 & 0 \\ 0 & 0 & 0 & e^{it\Delta} & 0 \\ 0 & 0 & 0 & 0 & e^{2it\Delta} \end{bmatrix}, \quad (27)$$

where  $\hat{U}_{\Delta=2\Omega_R}^{Split}$  is achieved by substituting  $\Delta = 2\Omega_R$ ,  $\Omega_G = \sqrt{5}\Omega_R$  and  $t = \frac{\pi}{\sqrt{5}\Omega_R}$  into Equation 14. Following on from Equation 7, the time evolution operator during free evolution  $\hat{U}_{\Omega_R=0}^{Free}$  is extrapolated as shown in Equation 25.

The equation for the system wavefunction at the end of the Ramsey sequence can be obtained by applying Equation 8

$$|\Psi_{sys}(t)\rangle = \begin{bmatrix} \frac{256}{625} \sin^4\left(\frac{\Delta t}{2}\right) \\ \frac{128}{625} \sin^3\left(\frac{\Delta t}{2}\right) \left(3 \sin\left(\frac{\Delta t}{2}\right) + 5i \cos\left(\frac{\Delta t}{2}\right)\right) \\ \frac{4\sqrt{6}}{625} (5i \sin(\Delta t) - 3 \cos(\Delta t) + 3)^2 \\ \frac{-4e^{-2i\Delta t}}{625} (-1 + e^{i\Delta t}) (4 + e^{i\Delta t})^3 \\ \frac{e^{-2i\Delta t}}{625} (4 + e^{i\Delta t})^4 \end{bmatrix}, P_{Rsy} = \begin{bmatrix} \frac{65536}{390625} \sin^8\left(\frac{\Delta t}{2}\right) \\ \frac{16384}{390625} \sin^6\left(\frac{\Delta t}{2}\right) (8 \cos(\Delta t) + 17) \\ \frac{1536}{390625} \sin^4\left(\frac{\Delta t}{2}\right) (8 \cos(\Delta t) + 17)^2 \\ \frac{64}{390625} \sin^2\left(\frac{\Delta t}{2}\right) (8 \cos(\Delta t) + 17)^3 \\ \frac{1}{390625} (8 \cos(\Delta t) + 17)^4 \end{bmatrix} \quad (28)$$

where  $|\Psi_{sys}(t)\rangle$  and  $P_{Rsy}$  are respectively the vector state and the populations for the five-level system at the end of the Ramsey sequence.

This can be converted to populations in Equation 28. Further, the Ramsey signal can be obtained when the average spin projection for a multilevel system  $\langle \hat{F}_Z \rangle = \hbar \sum_{m_F} m_F P_{m_F}$  is applied [10]. Based on  $\langle \hat{F}_Z \rangle$  the Ramsey signal takes the form  $\frac{\langle \hat{F}_Z \rangle}{\hbar} = \frac{2}{25} (9 + 16 \cos(\Delta t))$ . The importance of  $\Delta = 2\Omega_R$  scenario is that it denotes greater stability of the Rabi splitting after the pulse duration  $t = \frac{\pi}{\sqrt{5}\Omega_R}$  under experimental phase and pulse uncertainties. This is visible in Figure 6 showing minimal population variations of states  $|+1\rangle$  and  $|+2\rangle$  in the vicinity of equal splitting due to the flatness of the curves. Figure 7 shows the population variation and the Ramsey signal for  $\Delta = 2\Omega_R$ . A decreased interference fringe contrast is noticeable compared to a near-resonant case but we anticipate the measured interference signal will be more stable in the presence of magnetic and frequency noise.

### 3.3. Generalised Ramsey signal for the five-level system

As shown under Equation 14, the general form of the unitary time evolution operator  $\hat{U}$  can be derived which uses the important relation of  $\Delta = \alpha\Omega_R$  and the population at the end of the first splitting pulse is shown in Equation 16. Now, we look to expand the expression for  $\hat{U}$  (Equation 14) by generalising the variations in the pulse duration. This is important as it allows to account for the experimental uncertainty in pulse which leads to variations in the population splitting at both the EM pulses of the Ramsey sequence.

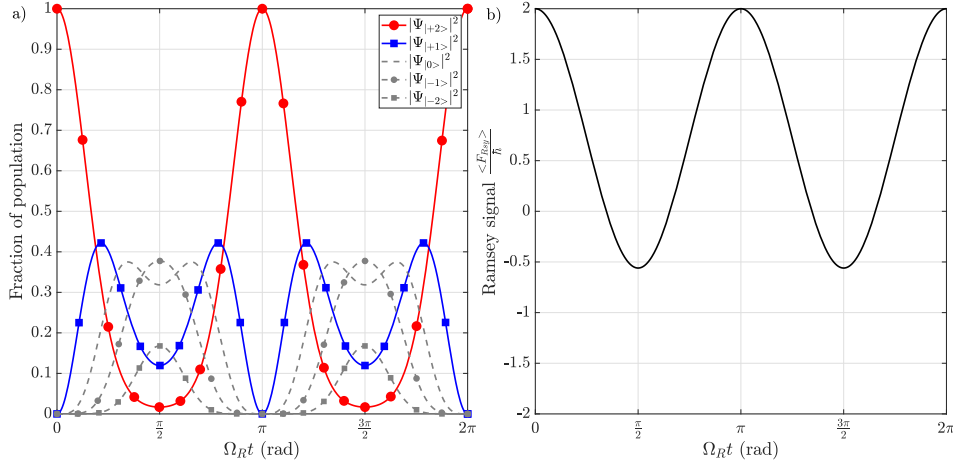


**Figure 7.** Population variations and the interference signal  $\frac{\langle \hat{F}_Z \rangle}{\hbar}$  after the Ramsey sequence for the case of  $\Delta = 2\Omega_R$  in the five-level system. **a)** The variation of the population of each state where the red solid line denotes  $|+2\rangle$  and the blue solid line denotes  $|+1\rangle$ . **b)** The variation of the Ramsey signal based on  $\frac{\langle \hat{F}_Z \rangle}{\hbar} = \sum_{m_F} m_F P_{m_F}$  where  $P_{m_F}$  is the population fraction of state  $|m_F\rangle$ .

To do so, the pulse duration can be defined as  $t = \frac{\beta}{\Omega_R}$ , where  $\beta$  is a phase relating to the pulse area defining the splitting of the system. This results in the following unitary time evolution operator

$$\hat{U}_{\alpha\beta}^{GSplit} = \begin{bmatrix} B_{11} & B_{12} & B_{13} & B_{14} & B_{15} \\ B_{12} & B_{22} & B_{23} & B_{24} & -B_{14}^* \\ B_{13} & B_{23} & B_{33} & -B_{23}^* & B_{13}^* \\ B_{14} & B_{24} & -B_{23}^* & B_{22}^* & -B_{12}^* \\ B_{15} & -B_{14}^* & B_{13}^* & -B_{12}^* & B_{11}^* \end{bmatrix}, \quad (29)$$

where  $\hat{U}_{\alpha\beta}^{GSplit}$  is achieved by substituting  $t = \frac{\beta}{\Omega_R}$  into Equation 14, where the full expressions are

$$\begin{aligned} B_{11} &= \frac{(8\alpha^2+4)\cos(\sqrt{\alpha^2+1}\beta) - 8i\alpha\sqrt{\alpha^2+1}\sin(\sqrt{\alpha^2+1}\beta)((2\alpha^2+1)\cos(\sqrt{\alpha^2+1}\beta)+1) + (8(\alpha^4+\alpha^2)+1)\cos(2\sqrt{\alpha^2+1}\beta)+3}{8(\alpha^2+1)^2} \\ B_{12} &= \frac{(4\alpha^2+3)\alpha\cos(2\sqrt{\alpha^2+1}\beta) + i(-2\sqrt{\alpha^2+1}\sin(\sqrt{\alpha^2+1}\beta)((4\alpha^2+1)\cos(\sqrt{\alpha^2+1}\beta)-2\alpha^2+1)+3i\alpha)-4\alpha^3\cos(\sqrt{\alpha^2+1}\beta)}{4(\alpha^2+1)^2} \\ B_{13} &= -\frac{\sqrt{\frac{3}{2}}\sin^2(\frac{1}{2}\sqrt{\alpha^2+1}\beta)(-2i\alpha\sqrt{\alpha^2+1}\sin(\sqrt{\alpha^2+1}\beta)+(2\alpha^2+1)\cos(\sqrt{\alpha^2+1}\beta)+1)}{(\alpha^2+1)^2} \\ B_{14} &= \frac{2\sin^3(\frac{1}{2}\sqrt{\alpha^2+1}\beta)(\alpha\sin(\frac{1}{2}\sqrt{\alpha^2+1}\beta)+i\sqrt{\alpha^2+1}\cos(\frac{1}{2}\sqrt{\alpha^2+1}\beta))}{(\alpha^2+1)^2} \\ B_{15} &= \frac{\sin^4(\frac{1}{2}\sqrt{\alpha^2+1}\beta)}{(\alpha^2+1)^2} \\ B_{22} &= \frac{(2\cos(\sqrt{\alpha^2+1}\beta)+\alpha^2-1)(-2i\alpha\sqrt{\alpha^2+1}\sin(\sqrt{\alpha^2+1}\beta)+(2\alpha^2+1)\cos(\sqrt{\alpha^2+1}\beta)+1)}{2(\alpha^2+1)^2} \\ B_{23} &= -\frac{\sqrt{6}\sin(\frac{1}{2}\sqrt{\alpha^2+1}\beta)(\cos(\sqrt{\alpha^2+1}\beta)+\alpha^2)(\alpha\sin(\frac{1}{2}\sqrt{\alpha^2+1}\beta)+i\sqrt{\alpha^2+1}\cos(\frac{1}{2}\sqrt{\alpha^2+1}\beta))}{(\alpha^2+1)^2} \\ B_{24} &= -\frac{\sin^2(\frac{1}{2}\sqrt{\alpha^2+1}\beta)(2\cos(\sqrt{\alpha^2+1}\beta)+3\alpha^2+1)}{(\alpha^2+1)^2} \\ B_{33} &= \frac{12\alpha^2\cos(\sqrt{\alpha^2+1}\beta)+3\cos(2\sqrt{\alpha^2+1}\beta)+(1-2\alpha^2)^2}{4(\alpha^2+1)^2} \end{aligned} \quad (30)$$



The wavefunction at the end of the Ramsey sequence can be obtained when  $\hat{U}_{\alpha\beta}^{GSplit}$  is applied to Equation 8, which can be converted to the population, which are omitted due to the immense lengths of the expressions. However, an expression for the Ramsey signal can be obtained when these populations are subjected to  $\frac{\langle \hat{F}_Z \rangle}{\hbar} = \sum_{m_F} m_F P_{m_F}$ , which results in a complete analytical expression for the average spin at the end of Ramsey interference in the five-level model:

$$\begin{aligned} \frac{\langle \hat{F}_Z \rangle}{\hbar} = & \frac{4\sqrt{\alpha^2+1}\alpha^2 \cos(\sqrt{\alpha^2+1}\beta) + \sqrt{\alpha^2+1} \cos(2\sqrt{\alpha^2+1}\beta) + (2\alpha^4+1)\sqrt{\alpha^2+1}}{(\alpha^2+1)^{5/2}} \\ & - \frac{4\sin^2\left(\frac{1}{2}\sqrt{\alpha^2+1}\beta\right) (\sqrt{\alpha^2+1} ((2\alpha^2+1)\cos(\sqrt{\alpha^2+1}\beta) + 1))}{(\alpha^2+1)^{5/2}} \cos(\Delta t) \\ & + \frac{4\sin^2\left(\frac{1}{2}\sqrt{\alpha^2+1}\beta\right) (2(\alpha^3+\alpha)\sin(\sqrt{\alpha^2+1}\beta))}{(\alpha^2+1)^{5/2}} \sin(\Delta t), \end{aligned} \quad (31)$$

where  $\alpha = \frac{\Delta}{\Omega_R}$  and  $\beta = \Omega_R t$ .

By using the trigonometric conversion of  $a \cos(\theta) + b \sin(\theta) = A \cos(\theta - \phi)$ , Equation 31 can be further simplified to the rather elegant form of:

$$\begin{aligned} \frac{\langle \hat{F}_Z \rangle}{\hbar} = & \frac{4\sqrt{\alpha^2+1}\alpha^2 \cos(\sqrt{\alpha^2+1}\beta) + \sqrt{\alpha^2+1} \cos(2\sqrt{\alpha^2+1}\beta) + (2\alpha^4+1)\sqrt{\alpha^2+1}}{(\alpha^2+1)^{5/2}} \\ & - \frac{4\sin^2\left(\frac{1}{2}\sqrt{\alpha^2+1}\beta\right) \left(\sqrt{(\alpha^2+1)} (\cos(\sqrt{\alpha^2+1}\beta) + 2\alpha^2 + 1)\right)}{(\alpha^2+1)^{5/2}} \cos(\Delta t - \phi). \end{aligned} \quad (32)$$

where  $\tan(\phi) = \frac{-2(\alpha^3+\alpha)\sin(\sqrt{\alpha^2+1}\beta)}{\sqrt{\alpha^2+1}((2\alpha^2+1)\cos(\sqrt{\alpha^2+1}\beta)+1)}$ .

The prominent feature is that Equation 32 reduces to  $\frac{\langle \hat{F}_Z \rangle}{\hbar} = A - B \cos(\Delta t - \phi)$  when values for  $\alpha$  and  $\beta$  are substituted. Further, the unique relation of  $A + B = 2$  is also reported. As a special note,  $\beta$  scans only within the first half of one Rabi cycle in the above analytical description. However, we scan the Rabi signal beyond one cycle in experiments; therefore,  $t = \frac{(2\pi+\beta)}{\Omega_R}$  or  $t = \frac{(4\pi-\beta)}{\Omega_R}$  should be used when converting a fitted  $\beta$  to experimental results.

#### 4. Discussion and conclusions

Here we have explored the analytical description of three- and five-level systems via unitary time evolution operators and obtained analytical expressions for describing the Ramsey interferometric signal for a typical Ramsey sequence. Several interesting Rabi oscillations for the three-level system are shown in Figure 1. Further, the behaviour of Rabi oscillations of the five-level system is verified via the expansion of expressions from the two-level model as shown in Figures 5 and 6. Several special cases and examples of how these analytical expressions can be used to obtain population variations along with the averaged Ramsey signal at the end of the Ramsey sequence are also presented as

shown in Figures 2 and 7. Finally, a generalised equation for the average Ramsey signal at the standard Ramsey sequence for the five-level system is presented in Equation 32 where the splitting condition is also generalised expanding the applicability.

A limitation of this analysis is that both splitting pulses of the Ramsey sequence are considered to be equal. However, this analysis can be expanded to Ramsey sequences with unequal splitting pulses by following the derivation methodology presented here. This means that a separate unitary time evolution operator  $\hat{U}$  is to be derived for the second pulse. From this the analytical expression for the system wavefunction at the end of the Ramsey sequence can be obtained via Equation 8. From this the populations of each state can be obtained from which the analytical expression for Ramsey interference can be obtained via  $\langle \hat{F}_Z \rangle = \hbar \sum_{m_F} m_F P_{m_F}$  where  $P_{m_F}$  is the fractional population of the relevant  $m_F$  state [10]. Similarly, this same methodology can be used to obtain analytical expressions for Ramsey sequences with spin-echo techniques such as for work reported in [19, 20, 21]. For this, a new unitary time evolution operator  $\hat{U}^\pi$  is to be derived for the  $\pi$ - pulse. Once Equation 8 is expanded to  $|\Psi_{sys}(t)\rangle = \hat{U}^{Split} \cdot \hat{U}^{Free} \cdot \hat{U}^\pi \cdot \hat{U}^{Free} \cdot \hat{U}^{Split} \cdot |\Psi(0)\rangle$ ; the analytical expression for the system wavefunction is obtained. From here, the analytical expression for the Ramsey interference is obtained by converting the system wavefunction to the multilevel populations.

All in all, a comprehensive analysis of the three- and five-level systems via the unitary time evolution operator under the equal-Rabi condition for a Ramsey sequence with equal splitting pulses is discussed.

## References

- [1] Ramsey N F 1990 *Science* **248** 1612–1619 URL <https://doi.org/10.1126/science.248.4963.1612>
- [2] Fang F, Li M, Lin P, Chen W, Liu N, Lin Y, Wang P, Liu K, Suo R and Li T 2015 *Metrologia* **52** 454–468 URL <https://doi.org/10.1088/0026-1394/52/4/454>
- [3] Heavner T P, Jefferts S R, Donley E A, Shirley J H and Parker T E 2005 *Metrologia* **42** 411–422 URL <https://doi.org/10.1088/0026-1394/42/5/012>
- [4] Peters A, Chung K Y and Chu S 1999 *Nature* **400** 849–852 URL <https://doi.org/10.1038/23655>
- [5] Rosi G, Sorrentino F, Cacciapuoti L, Prevedelli M and Tino G M 2014 *Nature* **510** 518–521 URL <https://doi.org/10.1038/nature13433>
- [6] Petrovic J, Herrera I, Lombardi P, Schäfer F and Cataliotti F S 2013 *New Journal of Physics* **15** 043002 URL <https://doi.org/10.1088/1367-2630/15/4/043002>
- [7] Anderson R P, Ticknor C, Sidorov A I and Hall B V 2009 *Physical Review A* **80** URL <https://doi.org/10.1103/physreva.80.023603>
- [8] Białynicka-Birula Z, Białynicki-Birula I, Eberly J H and Shore B W 1977 *Physical Review A* **16** 2048–2054 URL <https://doi.org/10.1103/physreva.16.2048>
- [9] Cook R J and Shore B W 1979 *Physical Review A* **20** 539–544 URL <https://doi.org/10.1103/physreva.20.539>
- [10] Anderson R 2010/11 *Nonequilibrium dynamics and relative phase evolution of two-component Bose-Einstein condensates* Ph.D. thesis Swinburne University of Technology
- [11] Vitanov N V and Suominen K A 1997 *Physical Review A* **56** R4377–R4380 URL <https://doi.org/10.1103/physreva.56.r4377>

- [12] Fujii K, Higashida K, Kato R and Wada Y 2003 URL <https://arxiv.org/abs/quant-ph/0307066>
- [13] Fujii K, Higashida K, Kato R and Wada Y 2004 URL <https://arxiv.org/abs/quant-ph/0312060>
- [14] Fujii K 2006 URL <https://arxiv.org/abs/quant-ph/0512126>
- [15] Steck D A 2019 Rubidium 87 d line data available online at <http://steck.us/alkalidata> revision 2.2.1
- [16] Breit G and Rabi I I 1931 *Physical Review* **38** 2082–2083 URL <https://doi.org/10.1103/physrev.38.2082.2>
- [17] Wu B, Wang Z, Cheng B, Wang Q, Xu A, Kong D and Lin Q 2014 *Journal of the Optical Society of America B* **31** 742 URL <https://doi.org/10.1364/josab.31.000742>
- [18] Majorana E 1932 *Il Nuovo Cimento* **9** 43–50 URL <https://doi.org/10.1007/bf02960953>
- [19] Eto Y, Sekine S, Hasegawa S, Sadgrove M, Saito H and Hirano T 2013 *Applied Physics Express* **6** 052801 URL <https://doi.org/10.7567/apex.6.052801>
- [20] Egorov M, Anderson R P, Ivannikov V, Opanchuk B, Drummond P, Hall B V and Sidorov A I 2011 *Physical Review A* **84** URL <https://doi.org/10.1103/physreva.84.021605>
- [21] Opanchuk B, Egorov M, Hoffmann S, Sidorov A I and Drummond P D 2012 *EPL (Europhysics Letters)* **97** 50003 URL <https://doi.org/10.1209/0295-5075/97/50003>